SCIENTIFIC REPORTS

OPEN

Human Polyclonal Antibodies Prevent Lethal Zika Virus Infection in Mice

Received: 23 December 2018
Accepted: 17 June 2019
Published online: 08 July 2019

Emilie Branche[1], Ayo Yila Simon[2], Nicholas Sheets[1], Kenneth Kim[1], Douglas Barker[2], Anh-Viet T. Nguyen[1], Harpreet Sahota[3], Matthew Perry Young[1], Rebecca Salgado[1], Anila Mamidi[1], Karla M. Viramontes[1], Trevor Carnelley[2], Hongyu Qiu[2], Annie Elong Ngono[1], Jose Angel Regla-Nava[1], Mercylia Xevana Susantono[1], Joan M. Valls Cuevas[1], Kieron Kennedy[2], Shantha Kodihalli[2] & Sujan Shresta[1]

Zika virus (ZIKV) is an emerging mosquito-borne flavivirus that represents a major threat to global health. ZIKV infections in adults are generally asymptomatic or present with mild symptoms. However, recent outbreaks of ZIKV have revealed that it can cause Congenital Zika Syndrome in neonates and Guillain-Barré syndrome in adults. Currently, no ZIKV-specific vaccines or antiviral treatments are available. In this study, we tested the efficacy of convalescent plasma IgG hyperimmune product (ZIKV-IG) isolated from individuals with high neutralizing anti-ZIKV titers as a therapeutic candidate against ZIKV infection using a model of ZIKV infection in *Ifnar1*$^{-/-}$ mice. ZIKV-IG successfully protected mice from lethal ZIKV challenge. In particular, ZIKV-IG treatment at 24 hours after lethal ZIKV infection improved survival by reducing weight loss and tissue viral burden and improving clinical score. Additionally, ZIKV-IG eliminated ZIKV-induced tissue damage and inflammation in the brain and liver. These results indicate that ZIKV-IG is efficacious against ZIKV, suggesting this human polyclonal antibody is a viable candidate for further development as a treatment against human ZIKV infection.

Zika virus (ZIKV) is an arthropod-borne virus belonging to the family *Flaviviridae*, similar to dengue, West Nile, Japanese encephalitis, and yellow fever viruses[1]. ZIKV was first identified in a sentinel rhesus monkey in the Zika Forest of Uganda in 1947 and was isolated from mosquitoes (*Aedes africanus*) in 1948[2]. ZIKV is transmitted through the bite of infected female *Ae. aegypti* mosquitoes[3] and potentially *Ae. albopictus* mosquitoes[4], as well as alternative non-vector routes which have been identified, including vertical (i.e., mother-to-infant)[5–8], transfusion[9–11], and sexual transmission[12]. From the 1950's to 1990's, serological evidence of ZIKV was reported in multiple Asian[13–16] and African[17–22] countries, but no outbreaks and only 14 cases of human ZIKV disease were described[17,22–25]. The first ZIKV outbreak was observed in 2007 on Yap Island in the Federated States of Micronesia[26], followed by a second outbreak in French Polynesia in 2013[27]. The most recent reported outbreak was on a larger scale that occurred from 2014 to 2016 in Latin America[28–30]. Interest in this virus increased after these outbreaks in part due to the emergence of ZIKV outside its previously known geographic range, showing the potential of the virus to spread wherever the mosquito vector is present. In addition, prior to the French Polynesia outbreak, ZIKV was known to be asymptomatic or cause only mild symptoms (fever, headache, malaise, arthralgia, myalgia, maculopapular rashes, and conjunctivitis). However, since 2007, severe complications of ZIKV infection, in particular Guillain–Barré Syndrome in adults[31,32] and Congenital Zika Syndrome in babies born to ZIKV-infected women[7,8,33–36] have been observed. These findings led the WHO to declare ZIKV a public health emergency of international concern in 2016 and expanded efforts for the development of vaccines and therapeutics to combat the disease.

Antibodies (Abs) have been shown to play a critical role in the protective immune response against infectious diseases and have been used for passive immunization, in the prevention and treatment of both bacterial and viral infections, for more than a century. Immune animal sera were first used in the late 1800's for treatment

[1]La Jolla Institute for Immunology 9420 Athena Circle, La Jolla, CA, 92037, USA. [2]Research and Development, Emergent BioSolutions Canada Inc, 155 Innovation Drive, Winnipeg, MB, R3T 5Y3, Canada. [3]Medical Affairs, Emergent BioSolutions Canada Inc, 155 Innovation Drive, Winnipeg, MB, R3T 5Y3, Canada. Correspondence and requests for materials should be addressed to S.K. (email: skodihalli@ebsi.com) or S.S. (email: sujan@lji.org)

of disease, followed by an era of immune human serum therapy for both viral and bacterial diseases. Notably, during the 1918 influenza pandemic, serum from recovered patients was used successfully to treat acutely ill patients[37]. The role of convalescent serum therapy expanded to many infections beyond influenza during the first half of the 20th century with clinical benefit demonstrated for other viral diseases like measles[38] and polio[39], and for invasive bacterial pathogens, including pneumococcus, *Haemophilus influenzae B*, and meningococcus[40,41]. Passive immunization with antibody-based therapies has emerged as a promising strategy for treating emerging infectious diseases, and include both monoclonal (mAb) and polyclonal antibodies (pAb), each of which has its advantages and disadvantages. For example, mAbs can be easily manufactured in large quantities and have a greater inherent biological consistency due to their epitope specificity as compared to pAbs. However, mAbs have limitations, including development of escape mutants and high production costs. In comparison with mAbs, pAbs can have more robust activities, neutralizing several virus strains even after viral mutations[42,43]. Although several studies have demonstrated that mAbs can provide therapeutic protection against ZIKV in various human and mouse models[44], only a single study to date has shown therapeutic potential of human pAbs produced from transchromosomal cows against ZIKV infection in mice. As no study has as yet assessed the efficacy of pAbs isolated from humans as a potential therapeutic against ZIKV, herein, we evaluate the therapeutic potential of a pAb preparation from human plasma containing high anti-ZIKV titers (ZIKV-IG).

Specifically, we used the *Ifnar1*$^{-/-}$ mouse model as a stringent challenge system to evaluate the therapeutic potential of ZIKV-IG. Prior to the recent ZIKV epidemics, only a few studies had been performed in mice and these required many serial passages of ZIKV in mice to produce consistent disease phenotypes[45–47]. Within the last three years, substantial efforts have been focused on generating new mouse models. ZIKV evades the anti-viral type I interferon (IFN) response, in part through inhibition of the STAT2 and STING pathways in human but not mouse cells[48–50]. This antagonism of the type I IFN receptor (Ifnar) signaling in a species-specific manner by ZIKV explains the more severe pathogenesis of ZIKV infection in mice with immature or compromised immune systems compared to adult immunocompetent mice, and why disruption of the Ifnar1 signaling increases susceptibility of mice to lethal ZIKV infection. Accordingly, wild type mice treated with blocking anti-*Ifnar1* mAb[51–54], and mice gene-deficient for *Ifnar1*[53–58] or for both *Ifnar1* and type II IFN receptors[59–61] have been widely used as models of ZIKV infection. We measured the effectiveness of ZIKV-IG therapy on survival, viral burden and tissue pathology in key organs, including spleen, kidneys, liver, sciatic nerves and brain, of *Ifnar1*$^{-/-}$ mice following lethal ZIKV challenge. ZIKV-IG treatment at 24 hrs post-infection increased survival by reducing viral burden and ZIKV-induced tissue damage and inflammation in several key organs. These findings demonstrated that a single dose of ZIKV-IG is efficacious against lethal Zika disease in a highly stringent mouse challenge model.

Results

ZIKV-IG decreases morbidity and mortality in a dose dependent manner in *Ifnar1*$^{-/-}$ mice. To evaluate the therapeutic efficacy of ZIKV-IG against ZIKV infection, *Ifnar1*$^{-/-}$ mice were infected with ZIKV (strain FSS13025, 1.0×10^3 FFU/mouse, retro-orbital (r.o.) route) and then treated with ZIKV-IG (50, 10, 2, 0.5 and 0.1 mg/kg, r.o. route) 24 hrs post-infection (p.i.). ZIKV-IG used for this study exhibits high neutralization activity against multiple ZIKV strains, including strain FSS13025 (Supplementary Fig. S1). Animals were observed daily for survival, body weight changes and clinical signs of disease for day 21 p.i. For the entire study, vehicle control has been used as a negative control because the outcomes for animals treated with vehicle control were not significantly different to those observed in animals treated with a naïve-ZIKV-IG placebo, and significant differences were observed between 50 mg/kg ZIKV-IG treated mice and both vehicle control ($p = 0.0022$) and naïve-ZIKV-IG ($p = 0.0022$) treated mice (Supplementary Fig. S2 and Table S1). A dose-dependent effect on mortality, weight changes and severity of ZIKV disease was observed in ZIKV-IG treated animals compared to those treated with vehicle control (Fig. 1). Specifically, mice treated with the highest dose of ZIKV-IG (50 mg/kg) displayed a 100% survival rate, which was significantly greater than controls (0% survival, $p = 0.0005$), and similarly high survival rate was observed in mice treated with 10 mg/kg as compared to control mice (87.5% survival, $p = 0.0042$). Survival rates in the lower dose groups of 25%, 0%, and 0% (2, 0.5 and 0.1 mg/kg, respectively) were not statistically different than for control animals (Fig. 1A and Table 1). Similar patterns were observed in analysis of median time to death, with statistically significant increases in median time to death compared to controls for the 50 mg/kg and 10 mg/kg dose groups ($p = 0.0001$ and $p = 0.0008$, respectively) but not for the lower dose groups (Table 2). As with mortality, the 50 mg/kg dose group showed reduced morbidity compared to the control group, with significantly different weight change and clinical score outcomes over the 21-day observation period (Fig. 1B,C). The 50 mg/kg dose group exhibited little to no weight loss and clinical signs of disease, while the 10 mg/kg dose group showed reduced morbidity compared to controls, but only in terms of clinical score outcomes (Fig. 1C) and not in terms of body weight (Fig. 1B). In contrast, the lowest dose groups (≤ 2 mg/kg) exhibited progressive deterioration of weight (Fig. 1B) and clinical score (Fig. 1C) beginning at day 6 p.i. and extending to time of death or severe disease necessitating euthanasia. These data indicate that the 50 mg/kg dose is the most efficacious of the doses tested against ZIKV infection in this mouse model.

ZIKV-IG treatment decreases viral replication and dissemination in *Ifnar1*$^{-/-}$ mice. To determine how ZIKV-IG treatment improves morbidity and mortality, we examined whether ZIKV-IG treatment reduces viral burden in sera and key target organs of ZIKV tropism (spleen, kidneys, liver, sciatic nerves, and brain). *Ifnar1*$^{-/-}$ mice were infected with ZIKV (strain FSS13025, 1.0×10^3 FFU/mouse, r.o. route) followed by treatment at 24 hrs p.i. with ZIKV-IG (50, 10, 2 and 0.5 mg/kg, r.o. route). Sera and organs were harvested on days 3 and 7 p.i., and levels of viral RNA and infectious virus to BHK cells were determined by qRT-PCR and FFA, respectively. The 0.1 mg/kg dose was not used in this experiment due to the observed similarities of mortality and morbidity between this group and the 0.5 mg/kg group. In the serum, only 50 mg/kg ZIKV-IG-treated

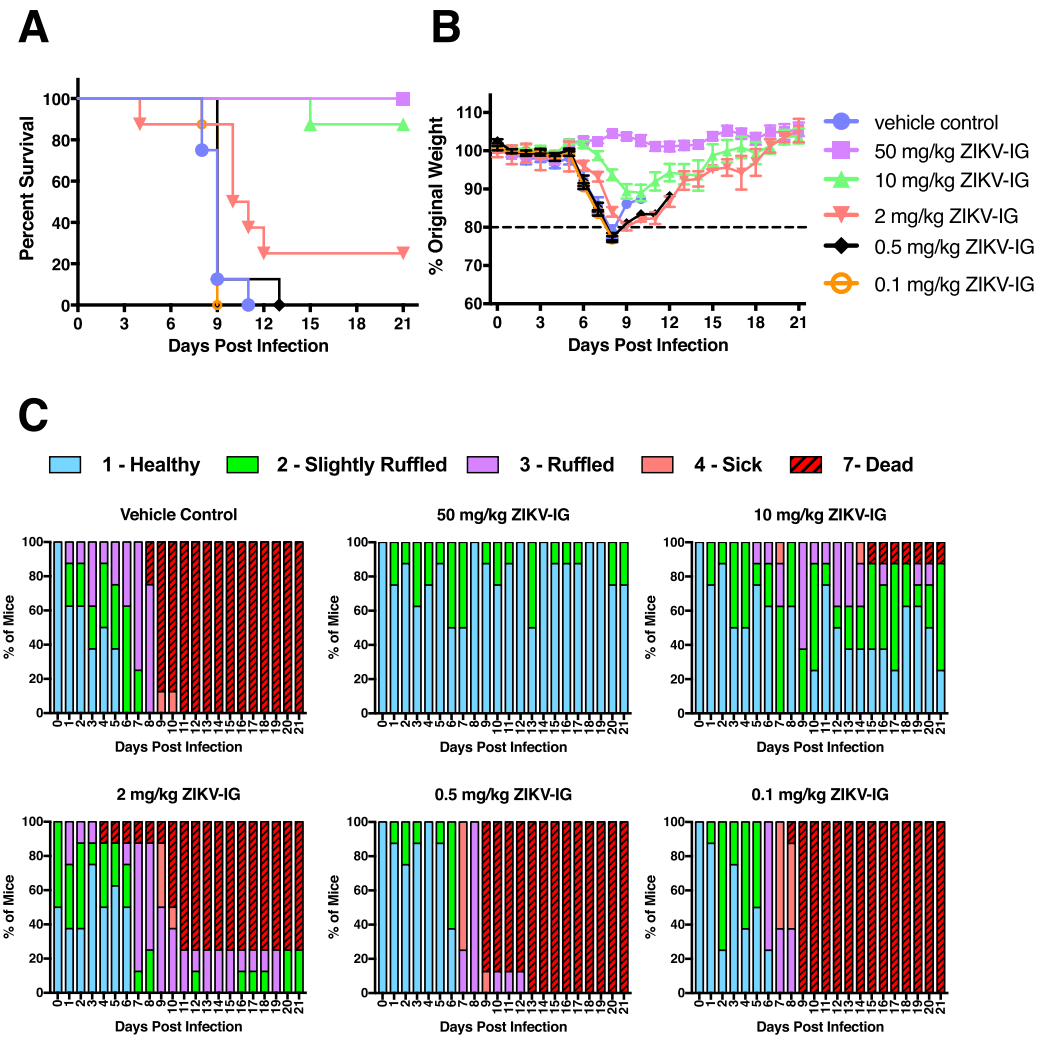

Figure 1. ZIKV-IG treatment improves survival of ZIKV-infected mice. Groups of *Ifnar1*$^{-/-}$ mice (n = 8) were infected with 1.0×10^3 FFU of ZIKV strain FSS13025 via a retro-orbital (r.o.) route. At 24 hrs p.i., mice were treated (via r.o. route) with vehicle, 50, 10, 2, 0.5 or 0.1 mg/kg ZIKV-IG. (**A**) Kaplan–Meier survival curves. (**B**) Mean percent weights, which are plotted for each group relative to the percent weight on day 0 (baseline). (**C**) Clinical scores. Error bars represent standard error of the mean.

Comparison to vehicle control			
Treatment Group	**% Survival**	**Fisher's Exact Test p-value**	**Bonferroni Adjusted p-value**
Vehicle control	0 (0/8)	NA	NA
50 mg/kg ZIKV-IG	100 (8/8)	0.00016**	0.0005**
10 mg/kg ZIKV-IG	87.5 (7/8)	0.00014**	0.0042**
2 mg/kg ZIKV-IG	25 (2/8)	0.467	1.000
0.5 mg/kg ZIKV-IG	0 (0/8)	NA	NA
0.1 mg/kg ZIKV-IG	0 (0/8)	NA	NA

Table 1. Analysis of survival rate between vehicle control group and ZIKV-IG-treated groups.

mice had significant reductions in both viral RNA (−1.1-fold, p = 0.017) and infectious virus levels (−1.8-fold, p = 0.043) at day 3 p.i. relative to vehicle-treated control mice (Fig. 2A and Supplementary Table S2). No significant reductions were noted in any animals treated with ≤10 mg/kg ZIKV-IG on day 3 p.i. or treated with any dose level on day 7 p.i. compared to controls, suggesting that by day 7 p.i. virus is cleared from circulation in all groups (Supplementary Fig. S3 and Table S2). In the spleen, similar levels of viral RNA and BHK cell-infectious viral particles were present in all groups at day 3 p.i., but at day 7 p.i., animals treated with 50 mg/

Comparison to vehicle control			
Treatment Group	**Median Survival (days)**	**Logrank Test p-value**	**Bonferroni Adjusted p-value**
Vehicle control	9	NA	NA
50 mg/kg ZIKV-IG	Undefined	<0.0001***	0.0001***
10 mg/kg ZIKV-IG	Undefined	<0.0001***	0.0008**
2 mg/kg ZIKV-IG	10.5	0.126	1.000
0.5 mg/kg ZIKV-IG	9	0.675	1.000
0.1 mg/kg ZIKV-IG	9	0.919	1.000

Table 2. Analysis of median time to death between vehicle control group and ZIKV-IG-treated groups.

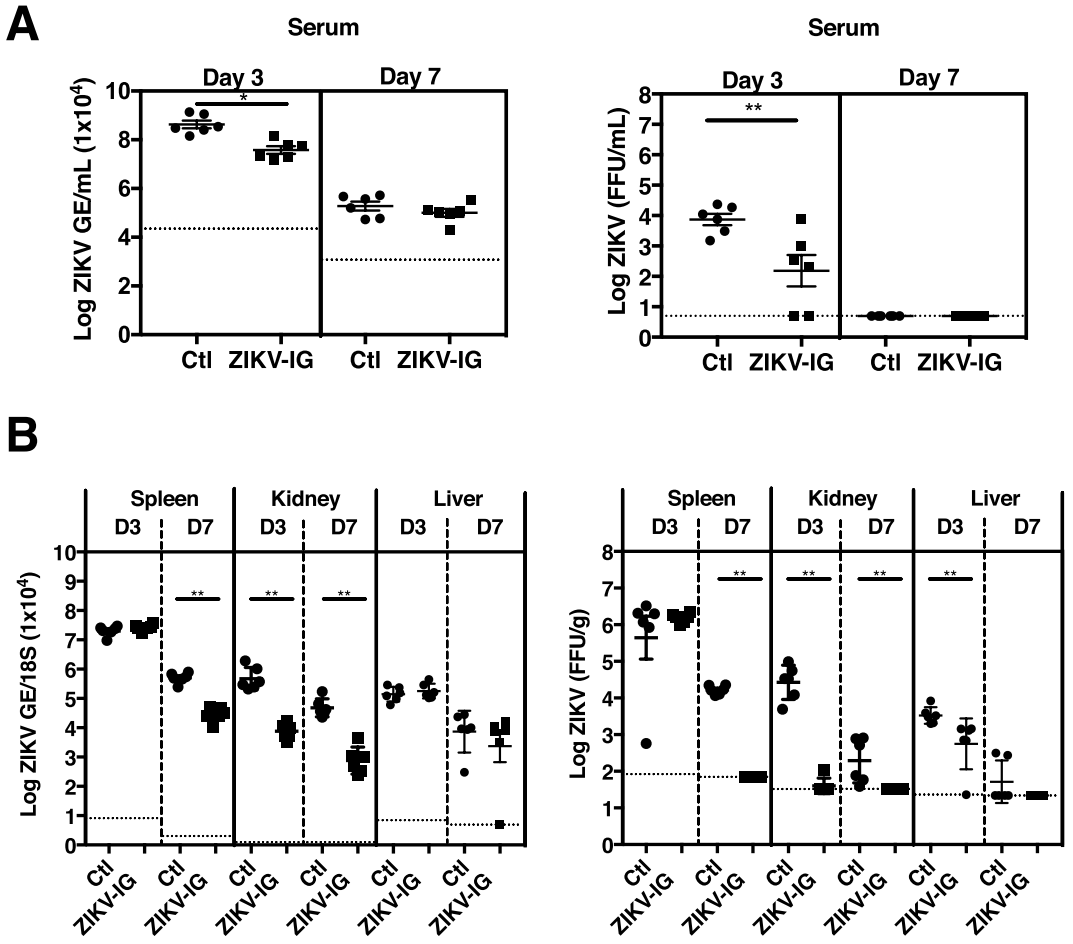

Figure 2. ZIKV-IG treatment decreases viral burden in key non-neuronal target organs of ZIKV in mice. Groups of *Ifnar1*$^{-/-}$ mice (n = 6) were infected with 1.0×10^3 FFU of ZIKV strain FSS13025 (via r.o. route). At 24 hrs p.i., mice were treated (r.o. route) with either vehicle (circles) or 50 mg/kg ZIKV-IG (squares). Viral RNA and infectious viral particle levels were determined by qRT-PCR and FFA, respectively, at days 3 and 7 p.i. in the (**A**) serum and (**B**) kidney, spleen and liver. Dotted lines indicate the limit of detection. The p values were obtained using non-parametric Wilcoxon Rank-Sum tests followed by the Bonferroni correction. Study groups were compared for statistical significance for each tissue and time-point. Error bars represent the standard error of the mean.

kg ZIKV-IG had lower levels of viral RNA (−1.3-fold, p = 0.009) and BHK cell-infectious virus (−2.3-fold, p = 0.009) relative to vehicle-treated control mice (Fig. 2B and Supplementary Table S2). Spleens of mice treated with 10 mg/kg ZIKV-IG (−1.3-fold, p = 0.009 for viral RNA and −1.7-fold, p = 0.009 for BHK cell-infectious ZIKV) and 2 mg/kg ZIKV-IG (−1.1-fold, p = 0.017 for viral RNA and −1.3-fold, p = 0.035 for infectious ZIKV) also contained lower levels of viral RNA and BHK cell-infectious virus than control mice at day 7 p.i. (Supplementary Fig. S3 and Table S2). In the kidney, 50 mg/kg ZIKV-IG treatment significantly reduced levels of viral RNA and BHK cell-infectious virus compared to controls at both day 3 p.i (−1.5-fold, p = 0.009 for viral RNA; −2.8-fold, p = 0.009 for infectious virus) and day 7 p.i. (−1.6-fold, p = 0.009 for viral RNA; −1.5-fold,

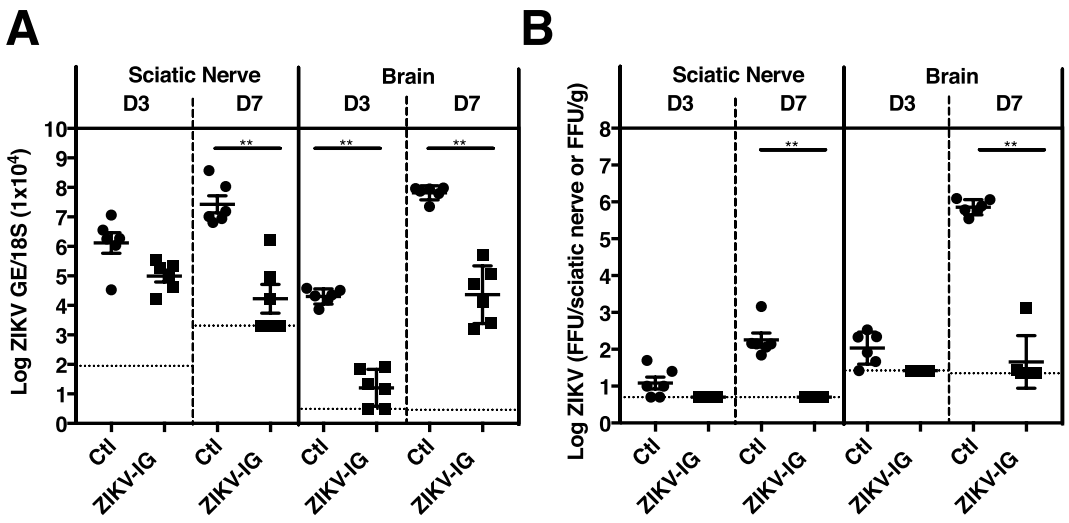

Figure 3. ZIKV-IG treatment decreases viral burden in the sciatic nerve and brain of ZIKV-infected mice. Groups of *Ifnar1*$^{-/-}$ mice (n = 6) were infected with 1.0×10^3 FFU of ZIKV strain FSS13025 (via r.o. route). At 24 hrs p.i., mice were treated (r.o. route) with vehicle (circle) or 50 (square) mg/kg ZIKV-IG. (**A**) ZIKV RNA levels, as measured by qRT-PCR and (**B**) infectious ZIKV levels, as determined by FFA analyses in the sciatic nerve and brain at days 3 and 7 p.i. Dotted lines indicate the limit of detection. Study groups were compared for statistical significance using Bonferroni corrected non-parametric Wilcoxon Rank-Sum tests for each tissue and time-point. Mean and standard error of the mean are shown.

p = 0.009 for infectious ZIKV) (Fig. 2B and Supplementary Table S2). Kidneys in animals treated with 10 mg/kg ZIKV-IG also contained decreased levels of viral RNA relative to control mice at day 3 p.i. (−1.1-fold, p = 0.035) (Supplementary Fig. S3 and Table S2). In the liver, 50 mg/kg ZIKV-IG-treated mice had similar levels of viral RNA but lower levels of BHK cell-infectious ZIKV (−1.3-fold, p = 0.009) than control mice at day 3 p.i. (Fig. 2B and Supplementary Table S2). At day 7 p.i., the liver RNA levels were significantly elevated in mice treated with 10 mg/kg (1.3-fold, p = 0.009), 2 mg/kg (1.5-fold, p = 0.009) and 0.5 mg/kg ZIKV-IG (1.3-fold, p = 0.017) as compared to control mice (Supplementary Fig. S3 and Table S2); however, no difference in levels of BHK cell-infectious virus was observed between the liver from any of the ZIKV-IG treated groups and control mice at day 7 p.i. (Supplementary Fig. S3 and Table S2). The increased viral RNA levels observed in the liver could be related to the analytical methods, as qRT-PCR detects viral RNA of both infectious and non-infectious virus particles, whereas the FFA analysis detects only BHK cell-infectious virus particles. Collectively, these results demonstrate that ZIKV-IG treatment reduces viral burden in key non-neuronal target tissues of ZIKV.

As the major consequences of ZIKV infection are related to infection of the nervous system, we next compared levels of viral RNA and BHK cell-infectious virus in the peripheral and central nervous system of ZIKV-IG-treated *vs*. control mice. At day 3 p.i., similar levels of ZIKV RNA and infectious particles were present in the sciatic nerves of control and ZIKV-IG-treated mice, but at day 7 p.i., both viral RNA (−2.6-fold, p = 0.009) and BHK cell-infectious ZIKV (−3.2-fold, p = 0.009) levels were reduced in the sciatic nerves of animals treated with 50 mg/kg ZIKV-IG relative to control mice (Fig. 3). Treatment with lower doses of ZIKV-IG also decreased levels of both viral RNA (2 mg/kg ZIKV-IG, −1.1-fold, p = 0.035) and BHK cell-infectious virus (10 mg/kg ZIKV-IG, −2.6-fold, p = 0.009) in the sciatic nerves at day 7 p.i (Supplementary Fig. S4 and Table S2). In the brain, 50 mg/kg ZIKV-IG treatment significantly reduced viral RNA levels at both days 3 and 7 p.i. (day 3 p.i. −4.1-fold, p = 0.009 and day 7 p.i. −1.8-fold, p = 0.009) relative to control mice (Fig. 3A and Supplementary Tables S2). Only low levels of BHK cell-infectious ZIKV were detected at day 3 p.i. in the brains of both 50 mg/kg ZIKV-IG and control groups. However, at day 7 p.i., control mouse brains carried high levels of BHK cell-infectious ZIKV, and the brains from 50 mg/kg ZIKV-IG-treated mice contained reduced levels of BHK cell-infectious ZIKV relative to control mice (−3.5-fold, p = 0.009) (Fig. 3B and Supplementary Table S2). Viral RNA (−1.3-fold, p = 0.009) and BHK cell-infectious ZIKV (−1.8-fold, p = 0.009) levels were also decreased the day 7 p.i. brains of mice treated with 10 mg/kg ZIKV-IG (Supplementary Fig. S4 and Table S2). These results are consistent with the sciatic nerves and brain being major target organs of ZIKV at a later time point post infection in this mouse model, and show that ZIKV-IG treatment reduces viral burden in both peripheral and central nervous tissues.

To confirm the robust efficacy of 50 mg/kg ZIKV-IG treatment against ZIKV infection in this mouse model, we next localized ZIKV in tissues by performing immunohistochemistry (IHC) for expression of ZIKV nonstructural protein 2B (NS2B), which is absent in virions and thus serves as a marker of viral replication. In the livers of control mice (Fig. 4Aa), NS2B was expressed in cells lining sinusoids that were morphologically consistent with liver sinusoidal endothelial cells and Kupffer cells (KC). In comparison, little to no NS2B immunoreactivity was seen in livers of mice treated with 50 mg/kg ZIKV-IG (Fig. 4Ab). Quantitative image analysis by ImageDx^{TM} software showed that median positive cell density in control mice was 7.55 cells/mm^2 relative to 0.13 cells/mm^2 in 50 mg/kg ZIKV-IG-treated mice (p = 0.006) (Fig. 4B). In the brain, NS2B was expressed in cells morphologically consistent with neurons and microglia in control mice (Fig. 4Ca), whereas little to no NS2B immunoreactivity

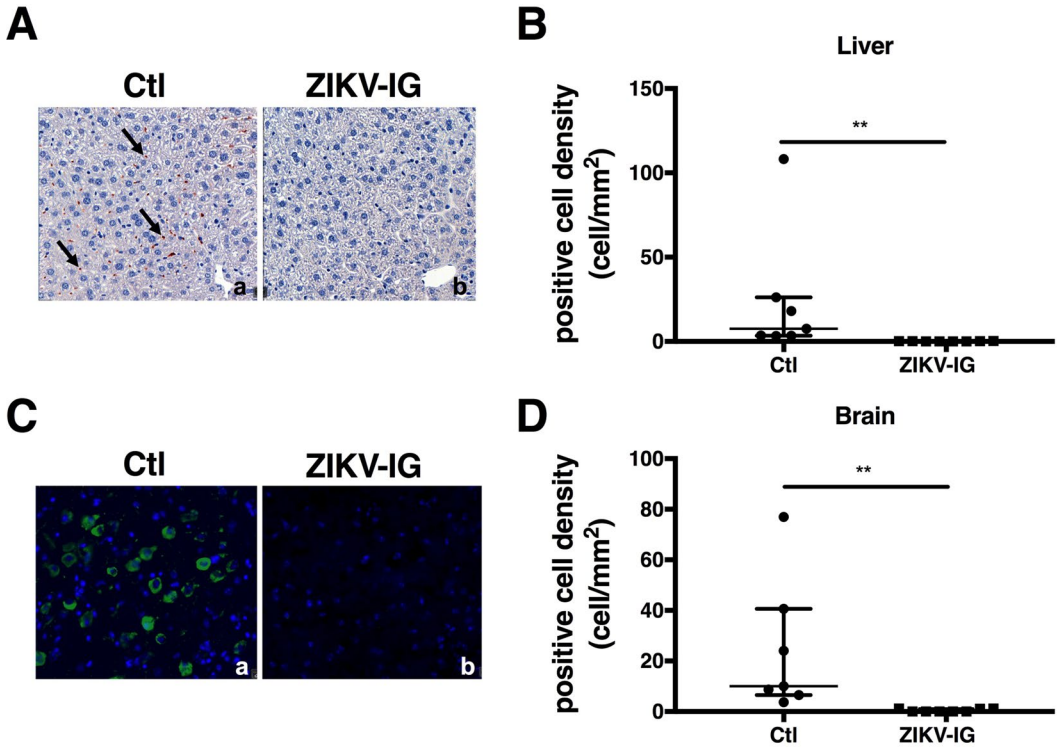

Figure 4. ZIKV-IG treatment decreases ZIKV NS2B expression in the liver and brain of ZIKV-infected mice. Groups of *Ifnar1*$^{-/-}$ mice (n = 8) were infected with 1.0×10^3 FFU of ZIKV strain FSS13025 (via r.o. route). At 24 hrs p.i., mice were treated (r.o. route) with vehicle or 50 mg/kg ZIKV-IG. At day 7 p.i., tissues were harvested to detect ZIKV NS2B expression via IHC. (**A**) NS2B expression in the liver (rust color dots, representative examples marked by arrows) of vehicle-treated mice after counterstaining with hematoxylin in cells morphologically consistent with LSECs and KCs. (**B**) NS2B expression in the liver was quantified using machine grading. (**C**) NS2B expression (green) was detected in vehicle-treated mice after counterstaining with DAPI in cells morphologically consistent with neurons and microglia. (**D**) NS2B expression was quantified using machine grading. Median and interquartile range are shown.

was seen in mice treated with 50 mg/kg ZIKV-IG (Fig. 4Cb). Quantitative analysis showed the median positive cell density in control mice was 10.88 cells/mm^2 as compared to 0.03 cells/mm^2 in 50 mg/kg ZIKV-IG-treated mice ($p = 0.006$) (Fig. 4D). Thus, 50 mg/kg ZIKV-IG treatment is effective against ZIKV infection in this highly stringent challenge model, as assessed via three different assays (qRT-PCR, FFA, and IHC). In particular, these results show that 50 mg/kg ZIKV-IG treatment reduces viral burden in multiple tissues of *Ifnar1*$^{-/-}$ mice at both the early (day 3) and late (day 7) time points after infection. In comparison to 50 mg/kg ZIKV-IG, lower doses of ZIKV-IG are less effective against ZIKV infection, reducing viral burden in select tissues.

ZIKV-IG treatment decreases ZIKV-induced brain pathology. ZIKV's neurotropism and associated brain pathology has been extensively documented in humans and *Ifnar1*$^{-/-}$ mice. Therefore, to evaluate the extent of brain tissue pathology and other signs of injury in ZIKV-IG-treated and control mice following ZIKV infection, hematoxylin & eosin-stained brain slide sections were examined and scored by a blinded board-certified pathologist. Scores for these sections are shown in Table 3. The most significant and severe lesions seen in the brains of the control group included nonsuppurative encephalitis, gliosis, nonsuppurative meningitis, neuronal necrosis, and malacia (Table 3 and Supplementary Fig. S5). In contrast, little or no pathology was observed in mice treated with 50 mg/kg ZIKV-IG. Thus, treatment with 50 mg/kg ZIKV-IG reduces ZIKV-induced brain pathology (Table 3 and Supplementary Fig. S5).

Discussion

In this study, we evaluated the therapeutic potential of human anti-ZIKV pAb (ZIKV-IG) against lethal ZIKV infection in a highly stringent mouse model. ZIKV-IG treatment was effective in protecting mice against ZIKV-induced mortality and morbidity by decreasing viral replication and dissemination into key target organs and ZIKV-induced pathology in the brain. These findings support further development of ZIKV-IG as a candidate for prophylaxis or treatment of Zika disease.

A variety of Abs, including mAbs isolated from ZIKV-immune individuals[62–64] and human polyclonal antibody produced in transchromosomal bovines[65] were shown to have therapeutic potential against ZIKV infection in mice. Similarly, transfer of convalescent sera from a human to pregnant mice prevented ZIKV infection and associated fetal birth defects[66], and convalescent human plasma or sera obtained from ZIKV-infected individuals were able to

	Treatment Group	Grading score for brain lesion per mouse (0 to +++)								Most frequent observed severity (average severity)
		m1	m2	m3	m4	m5	m6	m7	m8	
Nonsuppurative encephalitis	Ctl	++	++	++	++	+++	+++	+++	N/A	++ (2.43)
	50 mg/kg	0	0	0	0	0	+	+	+	0 (0.38)
Gliosis	Ctl	+	++	++	++	++	++	+++	N/A	++ (2.00)
	50 mg/kg	0	0	0	0	+	+	+	+	0/+ (0.50)
Nonsuppurative meningitis	Ctl	+	++	++	++	++	++	++	N/A	++ (1.86)
	50 mg/kg	0	0	0	0	0	0	0	+	0 (0.13)
Neural necrosis	Ctl	+	+	+	+	++	++	++	N/A	+ (1.43)
	50 mg/kg	0	0	0	0	0	+	+	+	0 (0.38)
Malacia	Ctl	0	0	+	+	+	+	+	N/A	+ (0.71)
	50 mg/kg	0	0	0	0	0	0	0	+	0 (0.13)
Hemorrhage	Ctl	0	0	0	0	0	+	+	N/A	0 (0)
	50 mg/kg	0	0	0	0	0	0	0	0	0 (0)

Table 3. Grading of brain histopathology.

neutralize both African and Asian ZIKV strains *in vitro*[67]. Here, we report that a single administration of 50 mg/kg human polyclonal Ab (ZIKV-IG) given at 24 hrs post-infection in *Ifnar1*$^{-/-}$ mouse model of lethal ZIKV infection prevented both severe disease development and mortality. In addition, ZIKV-IG reduced ZIKV burden and ZIKV-induced tissue damage in target organs, confirming therapeutic potential against ZIKV infection. Recent outbreaks of several emerging and re-emerging viral diseases for which no approved treatment or vaccine exists have rekindled interest in the development of plasma-derived immunoglobulin therapeutic products. In our current study, we used human polyclonal IgG antibodies purified from convalescent donor plasma containing high titers of anti-ZIKV Abs. Plasma collection was based on criteria set by FDA and Emergent's standards for virus screening and donor qualification. The immunoglobulin fraction was purified using a validated hyperimmune platform manufacturing process[68].

Although, ZIKV strains have been phylogenetically characterized into African and Asian/American lineages, the virus has very little genome variability and is classified as a single serotype[67]. This premise is supported by the report that primary infection with ZIKV African strain in macaques protected the animals from secondary heterologous re-challenge with ZIKV Asian strain[69]. Thus, an effective ZIKV therapeutic candidate could potentially neutralize infection with any of the ZIKV virus lineages. Our *in vitro* potency based on anti-ZIKV neutralization titer and *in vivo* mouse results provide evidence that ZIKV-IG can effectively neutralize ZIKV infection.

Development of Ab products intended for use as a therapy against ZIKV infection should consider the risk of antibody dependent enhancement (ADE) of infection, which has previously been described for dengue virus (DENV), another member of the family *Flaviviridae*[70–75]. During the ADE process, pre-existing non- or sub-neutralizing Abs that recognize DENV enhance subsequent DENV infection and pathogenesis[76–78]. ZIKV is antigenically and genetically similar to DENV with ~56% genome sequence homology[79], with *in vitro* and *in vivo* mouse studies demonstrating that Ab response to DENV and ZIKV can cross-react and cross-enhance infection and pathogenesis of each virus[79–83]. Although recent macaque and mouse studies have provided further support for pre-existing ZIKV Ab-mediated enhancement of subsequent DENV infection and disease severity[84–86], passive transfer of vaccine-induced Abs before ZIKV challenge did not result in ZIKV infection enhancement or disease in non-pregnant mice and monkeys[87,88]. Consistent with these studies[84–88], treatment with various sub-protective doses of ZIKV-IG showed no evidence for ADE of ZIKV infection in our mouse model as suggested by both survival and viral RNA results. No increase in mortality or viral burden were observed even using low ZIKV-IG concentrations which are potentially sub-neutralizing. However, viral load data obtained through focus forming assays using BHK cells may not be appropriate for drawing conclusions around the presence or absence of ADE as BHK cells lack expression of Fcγ receptors that support the ADE mode of infection.

Whether ADE is clinically relevant to human Zika disease is currently unknown, and thus, the possibility of ZIKV-IG-mediated ADE for Zika clinical disease remains a theoretical question for the development of Ab therapies against ZIKV. Further studies should be performed to assess whether ZIKV-IG has the potential to enhance DENV infection when given under pre-exposure setting.

In summary, we report that a single administration of 50 mg/kg of ZIKV-IG 24 hrs after infection protected mice against lethal ZIKV infection. Non-protective doses of ZIKV-IG did not induce ADE of ZIKV infection. These results provide the evidence that, at appropriate doses, ZIKV-IG treatment could be effective at preventing the deleterious effects of ZIKV in humans. Therefore, further testing in relevant pregnancy models to determine the impact of treatment on maternal and fetal infection is warranted.

Material and Methods

Key reagents, Abs, primers, and probes used in this study are outlined in Supplementary Table S3.

Virus. ZIKV strains MR766, FSS13025, and PRVABC59 were obtained from the World Reference Center for Emerging Viruses and Arboviruses (WRCEVA). FSS13025 is an Asian lineage strain isolated in 2010 from a pediatric case[89]. PRVABC59 is an Asian lineage strain isolated in 2015 from the blood of a human in Puerto Rico[90].

MR766 is an African lineage strain isolated in 1947 from a sentinel rhesus monkey (766) in Uganda[46]. Viruses were cultured using C6/36 *Aedes albopictus* mosquito cells, as described previously[91,92]. Virus was titrated using a baby hamster kidney (BHK)-21 cell-based focus-forming assay (FFA) as described previously[52].

Antibody neutralization assays. Naïve-ZIKV-IG and ZIKV-IG were initially diluted to 0.1 mg/mL and then serially diluted 1:3 for 11 dilutions in RPMI 1640 medium supplemented with 1% Hepes and 1% penicillin/streptomycin. Antibody dilutions were incubated at 37 °C with 5% CO_2 for 1 hr with either 1×10^5 FFU of ZIKV strain FSS13025, 2×10^4 FFU of ZIKV strain MR766, or 1×10^4 FFU of ZIKV strain PRVABC59. Standard flow cytometry-based neutralization assays using U937-DC-SIGN cells were then performed as described previously[58,86,93].

Mice and lethal ZIKV infection model. *Ifnar1*$^{-/-}$ mice (C57BL/6 mice deficient in type I interferon receptor) were originally obtained from Dr. W. Yokoyama (Washington University, St. Louis. MO) and subsequently bred under specific pathogen-free conditions at the animal facility of La Jolla Institute for Immunology. All experiments were approved by the Institutional Animal Care and Use Committee under protocol number AP028-SS1-0615/AP00001029. All experiments included age- and sex-matched mice. At 5–6 weeks of age, mice were randomized at first by gender and secondly per weight. Mice were inoculated intravenously *via* the retro-orbital (r.o.) route with 1.0×10^3 FFU of ZIKV FSS13025.

Testing of drug product and treatments. ZIKV-IG was a purified human IgG product manufactured using plasma collected from US FDA licensed plasma centers screened for Ab reactive to ZIKV. Established processes[68] were employed for manufacturing of ZIKV-IG (lot PD_740_ZKP_16_001_003_ER_v1) used in this study. This lot contained a total protein concentration of 54 mg/mL (>98.9% human IgG). Potency was determined using a microneutralization assay that measured the cytopathic effect of ZIKV strain PRVABC59 on Vero E6 cells using an xCELLigence® real-time cell analyzer (RTCA, ACEA Biosciences Inc.). Briefly, Vero E6 cells were added to an xCELLigence 96-well electronic microtiter plate (E-plate) then pre-incubated overnight at 37 °C in a humidified 5% CO_2 incubator. The E-plate contains electrodes in each well; adherent cells in the wells impede the electric current passing through the electrodes. An equal volume of ZIKV PRVABC59, diluted to 100 $TCID_{50}$, was incubated for one hour at 37 °C with serial dilutions of ZIKV-IG, then added to the E-plate. The E-plate was then incubated at 37 °C in an xCELLigence unit contained in a humidified 5% CO_2 incubator. Cells were monitored in real-time by measuring ZIKV-induced changes in cell impedance at 30-minute intervals. Sample dilution data from the defined end point was analyzed by fitting the impedance measure (cell index) to the log dilution using a 4-parameter logistic curve fit to determine the 50% neutralizing titer (NT_{50}). The initial potency value for ZIKV-IG product was 18,480, indicating a high degree of Zika virus neutralization.

Naïve-ZIKV-IG was manufactured using the same processes as ZIKV-IG, with the exception that the source plasma used did not contain Ab reactive to ZIKV. Mice were injected via r.o. route with 50, 10, 2.0, 0.5 or 0.1 mg/kg ZIKV-IG (100 μL/mouse) at 24 hrs following lethal ZIKV infection.

Clinical monitoring of mice and euthanasia criteria. Following infection, mice were weighed and observed for clinical signs and scored daily. Clinical scores were based on mouse appearance, mobility, and attitude on a 7-point scale (Table S3). Animals losing ≥20% body weight were humanely euthanized.

Viral quantification by qRT-PCR and Focus Forming Assay. *Sample collection.* Viral quantification was conducted by qRT-PCR and by Focus Forming Assay (FFA) on serum, spleen, kidney, liver, sciatic nerve, and brain. Sera were collected after centrifugation (15,900 g for 15 min at 4 °C) of blood harvested by cardiac puncture into collection tubes (Sarstedt, #41.1500.005). Following mouse perfusion with PBS, tissues were harvested and stored either in tubes containing RNA Later (Invitrogen) for qRT-PCR or in pre-weighed tubes containing MEMα medium and steel beads (Qiagen, #69989) for FFA. Tissues were then homogenized in RTL buffer (Qiagen) + 1% beta mercaptoethanol for qRT-PCR and MEMα medium for FFA followed by clarification (centrifugation at 2,000 × g for 5 min).

Viral RNA quantification by qRT-PCR. RNA from serum and homogenized tissues were isolated using the QIAmp Viral RNA Mini Kit (Qiagen) and the RNeasy Mini Kit (Qiagen), respectively. ZIKV RNA levels in sera and tissues were quantified by qRT-PCR. Specific primers and probes used are listed in Table S2. Tissue RNA levels were normalized to 18S as described for Dengue RNA[91] and expressed as genome equivalent per 18S (GE/18S), while serum RNA levels were expressed as GE/mL.

Quantification of infectious ZIKV by FFA. FFA procedures were performed as previously described[52]. Tissue samples were homogenized and clarified by centrifugation. Tissue supernatants and sera were diluted serially before infection on BHK cells. BHK cells used in this assay do not express Fcγ receptors. Cells were plated (2.0×10^5 cells/well in a 24-well plate) and incubated overnight at 37 °C, 5% CO_2. Confluent monolayers were inoculated with undiluted or 10-fold serially diluted sera or clarified tissue supernatant, and were incubated for 1 hr at 37 °C. After incubation, the inoculum was removed, and each cell monolayer was overlaid with CMC-media and incubated at 37 °C, 5% CO_2 for 1.5–2 days. Cells were then fixed, permeabilized, and incubated with pan *Flavivirus* anti-envelope (E) Ab clone 4G2 (BioXCell), followed by incubation with horseradish peroxidase-conjugated goat anti-mouse IgG secondary antibody (Jackson ImmunoResearch) and staining with True-Blue peroxidase substrate (Sera Care). Foci were counted, virus levels in the serum were expressed as Focus Forming Units (FFU) per mL, and for most tissues as FFU/g. As it was not technically feasible to weigh sciatic nerves, viral levels in these tissues were expressed as FFU/tissue.

Histopathology. At the time of necropsy, liver and brain were collected in 10% zinc formalin (BBC Biochemical) for histopathologic evaluation. Tissues were fixed for 48 hrs at room temperature. Brains were cut transversely at points corresponding to Bregma +2 mm and Bregma −3 mm of Mouse Brain Atlas celloidin case #170 (http://www.mbl.org), resulting in 3 brain sections (rostral, middle, and caudate). Tissues were processed routinely for paraffinization and cut at 4 μm thickness for H&E staining. Slides were blinded before review with an Olympus BX40 brightfield microscope at 2-60X magnification. Lesions were graded on a 4-point scale (0 to +++). All categories of lesions were tabulated (Table 3).

Enzyme immunohistochemistry. Paraffinized liver was cut onto slides (4 μm) and routinely deparaffinized. Slides were microwaved (GE, Model#: JES1142WD04) on high setting in Antigen Unmasking Solution (Vector Laboratories) and cooled at room temperature. Endogenous enzyme activity was blocked with BLOXALL (Vector Laboratories) and nonspecific protein binding was blocked with 10% Normal Goat Serum (Thermo Fisher). Slides were incubated with anti-ZIKV NS2B Ab (Genetex) at 4 °C for 14 hrs. Slides were incubated with ImmPRESS HRP (Vector Laboratories) secondary Ab followed by incubation with ImmPACT NovaRED (Vector Laboratories) substrate. Slides were counterstained with Modified Mayer's Hematoxylin (Thermo Fisher) and routinely processed for mounting. Positive, negative, and rabbit IgG (Vector Laboratories) controls were included with each batch. Morphology of immuno-reactive cells were confirmed by a board-certified pathologist, and immunoreactivity was quantified by ImageDx™ (Reveal Biosciences).

Immunofluorescence. At the time of necropsy, brains were collected in 4% paraformaldehyde (Alfa Aesar) at 4 °C and allowed to fix for 24 hrs. Tissues were then cryoprotected by serial immersion in 15% sucrose (Affymetrix) followed by 20% sucrose until the brains floated. Brains were cut transversely at points corresponding to Bregma +2 mm and Bregma −3 mm of Mouse Brain Atlas celloidin case #170 (http:/www.mbl.org). Tissues were transferred to cryomolds, embedded in OCT (Electron Microscopy Services), and frozen on dry ice followed by −80 °C freezer. Tissues were cut at 10 μm thickness for immunofluorescence. Slides were microwaved (GE, Model#: JES1142WD04) on high setting in Antigen Unmasking Solution (Vector Laboratories) and cooled at room temperature. Slides were incubated in Tris-Urea buffer and permeabilized with 0.1% Triton X-100 (Acros Organics). Nonspecific protein binding was blocked with 10% Horse Serum (Thermo Fisher). Slides were incubated with anti-ZIKV NS2B Ab (Genetex) at 4 °C for 14 hrs, followed by incubation with anti-rabbit AlexaFluor 488 (Invitrogen) secondary Ab and DAPI (Invitrogen) counterstain. Cover slips were mounted with Prolong Gold (Invitrogen). Positive, negative, and rabbit IgG (Vector Laboratories) controls were included with each batch. Morphology of cells in the brains was confirmed by a board-certified pathologist. Brain immunoreactivity was quantified by ImageDx™ (Reveal Biosciences).

Statistical analyses. Statistical analysis was performed using SAS version 9.3 statistical software (SAS). Survival rates and median time to death (MTD) were estimated using the Kaplan-Meier method. Data were analyzed either with Fisher's exact test (survival), Log-rank test (MTD) or exact Wilcoxon rank-sum test (viral RNA and infectious virus). All these tests were followed by a Bonferroni correction. Immunohistochemistry and immunofluorescence data for both brain and liver were analyzed with Kruskal-Wallis rank-sum test with Dwass, Steel, Critchlow-Fligner correction for multiple comparisons. Results were considered significant when $p < 0.05$.

References

1. Kuno, G., Chang, G. J., Tsuchiya, K. R., Karabatsos, N. & Cropp, C. B. Phylogeny of the genus Flavivirus. *J Virol* **72**, 73–83 (1998).
2. Dick, G. W., Kitchen, S. F. & Haddow, A. J. Zika virus. I. Isolations and serological specificity. *Trans R Soc Trop Med Hyg* **46**, 509–520 (1952).
3. Marchette, N. J., Garcia, R. & Rudnick, A. Isolation of Zika virus from Aedes aegypti mosquitoes in Malaysia. *Am J Trop Med Hyg* **18**, 411–415 (1969).
4. Grard, G. *et al.* Zika virus in Gabon (Central Africa)–2007: a new threat from Aedes albopictus? *PLoS Negl Trop Dis* **8**, e2681, https://doi.org/10.1371/journal.pntd.0002681 (2014).
5. Besnard, M., Lastere, S., Teissier, A., Cao-Lormeau, V. & Musso, D. Evidence of perinatal transmission of Zika virus, French Polynesia, December 2013 and February 2014. *Euro Surveill* **19** (2014).
6. Calvet, G. *et al.* Detection and sequencing of Zika virus from amniotic fluid of fetuses with microcephaly in Brazil: a case study. *Lancet Infect Dis* **16**, 653–660, https://doi.org/10.1016/S1473-3099(16)00095-5 (2016).
7. Mlakar, J. *et al.* Zika Virus Associated with Microcephaly. *N Engl J Med* **374**, 951–958, https://doi.org/10.1056/NEJMoa1600651 (2016).
8. Rasmussen, S. A., Jamieson, D. J., Honein, M. A. & Petersen, L. R. Zika Virus and Birth Defects–Reviewing the Evidence for Causality. *N Engl J Med* **374**, 1981–1987, https://doi.org/10.1056/NEJMsr1604338 (2016).
9. Barjas-Castro, M. L. *et al.* Probable transfusion-transmitted Zika virus in Brazil. *Transfusion* **56**, 1684–1688, https://doi.org/10.1111/trf.13681 (2016).
10. Motta, I. J. *et al.* Evidence for Transmission of Zika Virus by Platelet Transfusion. *N Engl J Med* **375**, 1101–1103, https://doi.org/10.1056/NEJMc1607262 (2016).
11. Musso, D. *et al.* Potential for Zika virus transmission through blood transfusion demonstrated during an outbreak in French Polynesia, November 2013 to February 2014. *Euro Surveill* **19** (2014).
12. Mead, P. S. *et al.* Zika Virus Shedding in Semen of Symptomatic Infected Men. *N Engl J Med* **378**, 1377–1385, https://doi.org/10.1056/NEJMoa1711038 (2018).
13. Smithburn, K. C. Neutralizing antibodies against arthropod-borne viruses in the sera of long-time residents of Malaya and Borneo. *Am J Hyg* **59**, 157–163 (1954).
14. Pond, W. L. Arthropod-Borne Virus Antibodies in Sera from Residents of South-East Asia. *Trans R Soc Trop Med Hyg* **57**, 364–371 (1963).
15. Darwish, M. A., Hoogstraal, H., Roberts, T. J., Ahmed, I. P. & Omar, F. A sero-epidemiological survey for certain arboviruses (Togaviridae) in Pakistan. *Trans R Soc Trop Med Hyg* **77**, 442–445 (1983).
16. Olson, J. G. *et al.* A survey for arboviral antibodies in sera of humans and animals in Lombok, Republic of Indonesia. *Ann Trop Med Parasitol* **77**, 131–137 (1983).
17. Simpson, D. I. Zika Virus Infection in Man. *Trans R Soc Trop Med Hyg* **58**, 335–338 (1964).

18. Jan, C., Languillat, G., Renaudet, J. & Robin, Y. A serological survey of arboviruses in Gabon. *Bull Soc Pathol Exot Filiales* **71**, 140–146 (1978).
19. Adekolu-John, E. O. & Fagbami, A. H. Arthropod-borne virus antibodies in sera of residents of Kainji Lake Basin, Nigeria 1980. *Trans R Soc Trop Med Hyg* **77**, 149–151 (1983).
20. Monlun, E. *et al.* Surveillance of the circulation of arbovirus of medical interest in the region of eastern Senegal. *Bull Soc Pathol Exot* **86**, 21–28 (1993).
21. Fagbami, A. Epidemiological investigations on arbovirus infections at Igbo-Ora, Nigeria. *Trop Geogr Med* **29**, 187–191 (1977).
22. Moore, D. L. *et al.* Arthropod-borne viral infections of man in Nigeria, 1964-1970. *Ann Trop Med Parasitol* **69**, 49–64 (1975).
23. Fagbami, A. H. Zika virus infections in Nigeria: virological and seroepidemiological investigations in Oyo State. *J Hyg (Lond)* **83**, 213–219 (1979).
24. Filipe, A. R., Martins, C. M. & Rocha, H. Laboratory infection with Zika virus after vaccination against yellow fever. *Arch Gesamte Virusforsch* **43**, 315–319 (1973).
25. Olson, J. G., Ksiazek, T. G., Suhandiman & Triwibowo Zika virus, a cause of fever in Central Java, Indonesia. *Trans R Soc Trop Med Hyg* **75**, 389–393 (1981).
26. Duffy, M. R. *et al.* Zika virus outbreak on Yap Island, Federated States of Micronesia. *N Engl J Med* **360**, 2536–2543, https://doi.org/10.1056/NEJMoa0805715 (2009).
27. Cao-Lormeau, V. M. *et al.* Zika virus, French Polynesia, South Pacific, 2013. *Emerg Infect Dis* **20**, 1085–1086, https://doi.org/10.3201/eid2006.140138 (2014).
28. Petersen, L. R., Jamieson, D. J., Powers, A. M. & Honein, M. A. Zika Virus. *N Engl J Med* **374**, 1552–1563, https://doi.org/10.1056/NEJMra1602113 (2016).
29. Zhang, Q. *et al.* Spread of Zika virus in the Americas. *Proc Natl Acad Sci USA* **114**, E4334–E4343, https://doi.org/10.1073/pnas.1620161114 (2017).
30. Colon-Gonzalez, F. J., Peres, C. A., Steiner Sao Bernardo, C., Hunter, P. R. & Lake, I. R. After the epidemic: Zika virus projections for Latin America and the Caribbean. *PLoS Negl Trop Dis* **11**, e0006007, https://doi.org/10.1371/journal.pntd.0006007 (2017).
31. Brasil, P. *et al.* Guillain-Barre syndrome associated with Zika virus infection. *Lancet* **387**, 1482, https://doi.org/10.1016/S0140-6736(16)30058-7 (2016).
32. Bautista, L. E. & Sethi, A. K. Association between Guillain-Barre syndrome and Zika virus infection. *Lancet* **387**, 2599–2600, https://doi.org/10.1016/S0140-6736(16)30844-3 (2016).
33. de Araujo, T. V. B. *et al.* Association between microcephaly, Zika virus infection, and other risk factors in Brazil: final report of a case-control study. *Lancet Infect Dis* **18**, 328–336, https://doi.org/10.1016/S1473-3099(17)30727-2 (2018).
34. Martines, R. B. *et al.* Pathology of congenital Zika syndrome in Brazil: a case series. *Lancet* **388**, 898–904, https://doi.org/10.1016/S0140-6736(16)30883-2 (2016).
35. Lucey, D., Cummins, H. & Sholts, S. Congenital Zika Syndrome in 2017. *JAMA* **317**, 1368–1369, https://doi.org/10.1001/jama.2017.1553 (2017).
36. Meneses, J. D. A. *et al.* Lessons Learned at the Epicenter of Brazil's Congenital Zika Epidemic: Evidence From 87 Confirmed Cases. *Clin Infect Dis* **64**, 1302–1308, https://doi.org/10.1093/cid/cix166 (2017).
37. Luke, T. C., Kilbane, E. M., Jackson, J. L. & Hoffman, S. L. Meta-analysis: convalescent blood products for Spanish influenza pneumonia: a future H5N1 treatment? *Ann Intern Med* **145**, 599–609 (2006).
38. Janeway, C. A. Use of Concentrated Human Serum gamma-Globulin in the Prevention and Attenuation of Measles. *Bull N Y Acad Med* **21**, 202–222 (1945).
39. Hammon, W. M., Coriell, L. L., Wehrle, P. F. & Stokes, J. Jr. Evaluation of Red Cross gamma globulin as a prophylactic agent for poliomyelitis. IV. Final report of results based on clinical diagnoses. *J Am Med Assoc* **151**, 1272–1285 (1953).
40. Alexander, H. E. *et al.* Hemophilus influenzae meningitis treated with streptomycin. *J Am Med Assoc* **132**, 434–440 (1946).
41. Casadevall, A. & Scharff, M. D. Serum therapy revisited: animal models of infection and development of passive antibody therapy. *Antimicrob Agents Chemother* **38**, 1695–1702 (1994).
42. Graham, B. S. & Ambrosino, D. M. History of passive antibody administration for prevention and treatment of infectious diseases. *Curr Opin HIV AIDS* **10**, 129–134, https://doi.org/10.1097/COH.0000000000000154 (2015).
43. Sparrow, E., Friede, M., Sheikh, M. & Torvaldsen, S. Therapeutic antibodies for infectious diseases. *Bull World Health Organ* **95**, 235–237, https://doi.org/10.2471/BLT.16.178061 (2017).
44. Wang, Q., Yan, J. & Gao, G. F. Monoclonal Antibodies against Zika Virus: Therapeutics and Their Implications for Vaccine Design. *J Virol* **91**, https://doi.org/10.1128/JVI.01049-17 (2017).
45. Bell, T. M., Field, E. J. & Narang, H. K. Zika virus infection of the central nervous system of mice. *Arch Gesamte Virusforsch* **35**, 183–193 (1971).
46. Dick, G. W. Zika virus. II. Pathogenicity and physical properties. *Trans R Soc Trop Med Hyg* **46**, 521–534 (1952).
47. Way, J. H., Bowen, E. T. & Platt, G. S. Comparative studies of some African arboviruses in cell culture and in mice. *J Gen Virol* **30**, 123–130, https://doi.org/10.1099/0022-1317-30-1-123 (1976).
48. Grant, A. *et al.* Zika Virus Targets Human STAT2 to Inhibit Type I Interferon Signaling. *Cell Host Microbe* **19**, 882–890, https://doi.org/10.1016/j.chom.2016.05.009 (2016).
49. Kumar, A. *et al.* Zika virus inhibits type-I interferon production and downstream signaling. *EMBO Rep* **17**, 1766–1775, https://doi.org/10.15252/embr.201642627 (2016).
50. Ding, Q. *et al.* Species-specific disruption of STING-dependent antiviral cellular defenses by the Zika virus NS2B3 protease. *Proc Natl Acad Sci USA* **115**, E6310–E6318, https://doi.org/10.1073/pnas.1803406115 (2018).
51. Govero, J. *et al.* Zika virus infection damages the testes in mice. *Nature* **540**, 438–442, https://doi.org/10.1038/nature20556 (2016).
52. Elong Ngono, A. *et al.* Mapping and Role of the CD8(+) T Cell Response During Primary Zika Virus Infection in Mice. *Cell Host Microbe* **21**, 35–46, https://doi.org/10.1016/j.chom.2016.12.010 (2017).
53. Wen, J. *et al.* Dengue virus-reactive CD8(+) T cells mediate cross-protection against subsequent Zika virus challenge. *Nat Commun* **8**, 1459, https://doi.org/10.1038/s41467-017-01669-z (2017).
54. Regla-Nava, J. A. *et al.* Cross-reactive Dengue virus-specific CD8(+) T cells protect against Zika virus during pregnancy. *Nat Commun* **9**, 3042, https://doi.org/10.1038/s41467-018-05458-0 (2018).
55. Lazear, H. M. *et al.* A Mouse Model of Zika Virus Pathogenesis. *Cell Host Microbe* **19**, 720–730, https://doi.org/10.1016/j.chom.2016.03.010 (2016).
56. Miner, J. J. *et al.* Zika Virus Infection during Pregnancy in Mice Causes Placental Damage and Fetal Demise. *Cell* **165**, 1081–1091, https://doi.org/10.1016/j.cell.2016.05.008 (2016).
57. Miner, J. J. *et al.* Zika Virus Infection in Mice Causes Panuveitis with Shedding of Virus in Tears. *Cell Rep* **16**, 3208–3218, https://doi.org/10.1016/j.celrep.2016.08.079 (2016).
58. Wen, J. *et al.* Identification of Zika virus epitopes reveals immunodominant and protective roles for dengue virus cross-reactive CD8(+) T cells. *Nat Microbiol* **2**, 17036, https://doi.org/10.1038/nmicrobiol.2017.36 (2017).
59. Dowall, S. D. *et al.* A Susceptible Mouse Model for Zika Virus Infection. *PLoS Negl Trop Dis* **10**, e0004658, https://doi.org/10.1371/journal.pntd.0004658 (2016).
60. Rossi, S. L. *et al.* Characterization of a Novel Murine Model to Study Zika Virus. *Am J Trop Med Hyg* **94**, 1362–1369, https://doi.org/10.4269/ajtmh.16-0111 (2016).

61. Tang, W. W. *et al*. A Mouse Model of Zika Virus Sexual Transmission and Vaginal Viral Replication. *Cell Rep* **17**, 3091–3098, https://doi.org/10.1016/j.celrep.2016.11.070 (2016).
62. Wang, Q. *et al*. Molecular determinants of human neutralizing antibodies isolated from a patient infected with Zika virus. *Sci Transl Med* **8**, 369ra179, https://doi.org/10.1126/scitranslmed.aai8336 (2016).
63. Sapparapu, G. *et al*. Neutralizing human antibodies prevent Zika virus replication and fetal disease in mice. *Nature* **540**, 443–447, https://doi.org/10.1038/nature20564 (2016).
64. Li, C. *et al*. A Single Injection of Human Neutralizing Antibody Protects against Zika Virus Infection and Microcephaly in Developing Mouse Embryos. *Cell Rep* **23**, 1424–1434, https://doi.org/10.1016/j.celrep.2018.04.005 (2018).
65. Stein, D. R. *et al*. Human polyclonal antibodies produced in transchromosomal cattle prevent lethal Zika virus infection and testicular atrophy in mice. *Antiviral Res* **146**, 164–173, https://doi.org/10.1016/j.antiviral.2017.09.005 (2017).
66. Wang, S. *et al*. Transfer of convalescent serum to pregnant mice prevents Zika virus infection and microcephaly in offspring. *Cell Res* **27**, 158–160, https://doi.org/10.1038/cr.2016.144 (2017).
67. Dowd, K. A. *et al*. Broadly Neutralizing Activity of Zika Virus-Immune Sera Identifies a Single Viral Serotype. *Cell Rep* **16**, 1485–1491, https://doi.org/10.1016/j.celrep.2016.07.049 (2016).
68. Kammanadiminti, S. *et al*. Combination therapy with antibiotics and anthrax immune globulin intravenous (AIGIV) is potentially more effective than antibiotics alone in rabbit model of inhalational anthrax. *PLoS One* **9**, e106393, https://doi.org/10.1371/journal.pone.0106393 (2014).
69. Aliota, M. T. *et al*. Heterologous Protection against Asian Zika Virus Challenge in Rhesus Macaques. *PLoS Negl Trop Dis* **10**, e0005168, https://doi.org/10.1371/journal.pntd.0005168 (2016).
70. Guzman, M. G. *et al*. Enhanced severity of secondary dengue-2 infections: death rates in 1981 and 1997 Cuban outbreaks. *Rev Panam Salud Publica* **11**, 223–227 (2002).
71. Halstead, S. B. *In vivo* enhancement of dengue virus infection in rhesus monkeys by passively transferred antibody. *J Infect Dis* **140**, 527–533 (1979).
72. Tamura, M., Webster, R. G. & Ennis, F. A. Subtype cross-reactive, infection-enhancing antibody responses to influenza A viruses. *J Virol* **68**, 3499–3504 (1994).
73. Sauter, P. & Hober, D. Mechanisms and results of the antibody-dependent enhancement of viral infections and role in the pathogenesis of coxsackievirus B-induced diseases. *Microbes Infect* **11**, 443–451 (2009).
74. Takada, A., Ebihara, H., Feldmann, H., Geisbert, T. W. & Kawaoka, Y. Epitopes required for antibody-dependent enhancement of Ebola virus infection. *J Infect Dis* **196**(Suppl 2), S347–356, https://doi.org/10.1086/520581 (2007).
75. Willey, S. *et al*. Extensive complement-dependent enhancement of HIV-1 by autologous non-neutralising antibodies at early stages of infection. *Retrovirology* **8**, 16, https://doi.org/10.1186/1742-4690-8-16 (2011).
76. Whitehead, S. S., Blaney, J. E., Durbin, A. P. & Murphy, B. R. Prospects for a dengue virus vaccine. *Nat Rev Microbiol* **5**, 518–528, https://doi.org/10.1038/nrmicro1690 (2007).
77. Burke, D. S., Nisalak, A., Johnson, D. E. & Scott, R. M. A prospective study of dengue infections in Bangkok. *Am J Trop Med Hyg* **38**, 172–180 (1988).
78. Halstead, S. B. Neutralization and antibody-dependent enhancement of dengue viruses. *Adv Virus Res* **60**, 421–467 (2003).
79. Barba-Spaeth, G. *et al*. Structural basis of potent Zika-dengue virus antibody cross-neutralization. *Nature* **536**, 48–53, https://doi.org/10.1038/nature18938 (2016).
80. Dejnirattisai, W. *et al*. Dengue virus sero-cross-reactivity drives antibody-dependent enhancement of infection with zika virus. *Nat Immunol* **17**, 1102–1108, https://doi.org/10.1038/ni.3515 (2016).
81. Priyamvada, L. *et al*. Human antibody responses after dengue virus infection are highly cross-reactive to Zika virus. *Proc Natl Acad Sci USA* **113**, 7852–7857, https://doi.org/10.1073/pnas.1607931113 (2016).
82. Stettler, K. *et al*. Specificity, cross-reactivity, and function of antibodies elicited by Zika virus infection. *Science* **353**, 823–826, https://doi.org/10.1126/science.aaf8505 (2016).
83. Bardina, S. V. *et al*. Enhancement of Zika virus pathogenesis by preexisting antiflavivirus immunity. *Science* **356**, 175–180, https://doi.org/10.1126/science.aal4365 (2017).
84. George, J. *et al*. Prior Exposure to Zika Virus Significantly Enhances Peak Dengue-2 Viremia in Rhesus Macaques. *Sci Rep* **7**, 10498, https://doi.org/10.1038/s41598-017-10901-1 (2017).
85. Watanabe, S., Tan, N. W. W., Chan, K. W. K. & Vasudevan, S. G. Dengue and Zika Virus Serological Cross-reactivity and their Impact on Pathogenesis in Mice. *J Infect Dis*. https://doi.org/10.1093/infdis/jiy482 (2018).
86. Fowler, A. M. *et al*. Maternally Acquired Zika Antibodies Enhance Dengue Disease Severity in Mice. *Cell Host Microbe* **24**, 743–750 e745, https://doi.org/10.1016/j.chom.2018.09.015 (2018).
87. Abbink, P. *et al*. Protective efficacy of multiple vaccine platforms against Zika virus challenge in rhesus monkeys. *Science* **353**, 1129–1132, https://doi.org/10.1126/science.aah6157 (2016).
88. Larocca, R. A. *et al*. Vaccine protection against Zika virus from Brazil. *Nature* **536**, 474–478, https://doi.org/10.1038/nature18952 (2016).
89. Heang, V. *et al*. Zika virus infection, Cambodia, 2010. *Emerg Infect Dis* **18**, 349–351, https://doi.org/10.3201/eid1802.111224 (2012).
90. Lanciotti, R. S., Lambert, A. J., Holodniy, M., Saavedra, S. & Signor Ldel, C. Phylogeny of Zika Virus in Western Hemisphere, 2015. *Emerg Infect Dis* **22**, 933–935, https://doi.org/10.3201/eid2205.160065 (2016).
91. Prestwood, T. R., Prigozhin, D. M., Sharar, K. L., Zellweger, R. M. & Shresta, S. A mouse-passaged dengue virus strain with reduced affinity for heparan sulfate causes severe disease in mice by establishing increased systemic viral loads. *J Virol* **82**, 8411–8421, https://doi.org/10.1128/JVI.00611-08 (2008).
92. Prestwood, T. R. *et al*. Trafficking and replication patterns reveal splenic macrophages as major targets of dengue virus in mice. *J Virol* **86**, 12138–12147, https://doi.org/10.1128/JVI.00375-12 (2012).
93. Elong Ngono, A. *et al*. CD4+ T cells promote humoral immunity and viral control during Zika virus infection. *PLoS Pathog* **15**, e1007474, https://doi.org/10.1371/journal.ppat.1007474 (2019).

Acknowledgements

This research was supported by Emergent BioSolutions Canada Inc, Winnipeg, Canada. The animal studies described herein were conducted in accordance with the approval of the Institutional Animal Care and Use Committee of La Jolla Institute for Immunology (Protocol # AP028-SS1-0615/AP00001029).

Author Contributions

E.B., A.Y.S., S.K. and S.S. conceived the project. E.B., A.Y.S. and S.K. designed experiments. E.B., N.S., K.K., A.T.N., M.P.Y., R.S., K.M.V., A.M., A.E.N., J.A.R.N., M.X.S. and J.V.C. performed experiments. E.B., A.T.N., M.P.Y., A.M., K.V., A.Y.S. and H.Q. performed quality control data screening. E.B. and A.T.N. performed the data analysis. T.C. and K.K. led the development and execution of ZIKV-IG characterization assays. H.S. performed the statistical analyses. E.B., A.Y.S. and K.K. wrote the manuscript. H.Q., D.B., S.K. and S.S. edited the manuscript.

Additional Information

Supplementary information accompanies this paper at https://doi.org/10.1038/s41598-019-46291-9.

Competing Interests: The study has been funded by Emergent BioSolutions Canada Inc, Winnipeg, Canada. AYE, DB, HQ, TC, HS and SK are employees of Emergent BioSolutions. EB, NS, KK, ATN, MPY, RS, KMV, AM, AEN, JARN, MXS and JVC and SS are employees of La Jolla Institute for Immunology who received funding to perform the work described.

Publisher's note: Springer Nature remains neutral with regard to jurisdictional claims in published maps and institutional affiliations.